AIAA JOURNAL
Vol. 36, No. 7, July 1998

Compressive Behavior of Multiply Delaminated Composite Laminates Part 2: Finite Element Analysis

Hiroshi Suemasu* and Tatsuya Kumagai†
Sophia University, Tokyo 102, Japan

Postbuckling behavior of rectangular composite plates with multiple circular delaminations is studied numerically using finite element analysis. Embedded circular delaminations are placed at regular intervals in the thickness direction at the plate center. The plate is fixed along its loading edges and simply supported at its side edges. The three-dimensional block element is adopted to accurately obtain distributions of energy release rates G_I, G_{II}, and G_{III}, along the delamination fronts based on the virtual crack closure technique. The contact problem of the delaminated surface is considered through introducing a spring element between nodes at the upper and lower surfaces of the delaminations, which resist only compression force. Buckling loads obtained in the present analysis agree well with those obtained from experiment and classical Rayleigh–Ritz analysis (see companion paper). The complex compressive behavior observed in the experiment can be explained through the results obtained in the present finite element method, which strongly depends on initial imperfections. The distribution of energy release rates in the postbuckling region is also consistent with the failure of the delaminated laminates observed in the experiment.

I. Introduction

THE compression after impact (CAI) problem, that is, the compressive strength of composite laminates significantly reduces due to damage as a result of low-velocity impact of a foreign object, is one of the most important issues in the design of composite structures because decreased compressive strength is often a critical concern. Because delamination below the impact point is thought to be the main reason for a significant reduction in the compressive strength of composite laminates, the effect of delamination(s) on the buckling and postbuckling properties of composite laminates has been studied analytically and experimentally by many researchers. The finite element method has often been applied to the problems of buckling, postbuckling, and stability of delamination crack(s) in postbuckling behavior, due to its effectiveness in handling problems with complex conditions, such as contact condition. One-dimensional, beam-type models of delaminated laminates have been studied by several researchers, including Wang et al.,[1] Suemasu et al.,[2] Davidson and Krafchak,[3] and Lee et al.,[4] using finite element analysis to investigate postbuckling behavior and the stability of the delaminations inasmuch as the problem is, at most, two dimensional in nature and, thus, does not require excessive numerical effort. These studies have shown the validity of the numerical method for application to this class of problem, including nonlinear analysis, the contact problem, and obtainment of the fracture mechanical parameter of the energy release rate. Limited research has been conducted toward the two-dimensional plate problem, however, as two-dimensional modeling of a delaminated plate requires a large numerical effort, particularly when the delamination crack stability is discussed. Whitcomb and Shivakumar[5] studied such a problem using the assumption of a surface delamination, whereas Shahwan and Waas[6] investigated the postbuckling behavior of a surface delamination considering the contact problem. Klug et al.[7] studied the postbuckling behavior of a plate with an elliptical delamination using the plate finite element and discussed the stability problem of the delamination by considering the energy release rate distribution.

Impact tests, e.g., Refs. 8–11, showed that multiple delaminations, being relatively small compared to the size of the plate, were produced at the impact point of CF/epoxy plates, with the compressive strength of the damaged plate being reduced to approximately one-third of its virgin state. The main cause of reduced compressive strength due to impact is believed to be the existence of multiple delaminations. Thus, the effect of multiple delaminations on the compressive behavior of composite plates needs to be understood.

Suemasu et al.[12] studied the effect of multiple delaminations on the compressive behavior of rectangular plates through a buckling analysis using the Rayleigh–Ritz method together with experimental observations. The experiment showed that the instability of delamination cracks could be a trigger for the final failure of the delaminated plate, and this depends on the plate dimensions, delamination size, interlaminar toughness, etc. Although the reduction in the buckling load could be adequately explained using the Rayleigh–Ritz analysis, the postbuckling behavior and delamination stability in multiply delaminated plates must also be studied to predict the CAI strength. In the present paper, the effect of multiple circular delaminations on the compressive behavior and instability of delamination cracks is discussed using finite element results and compared with experimental results obtained in a companion paper.[12]

II. Finite Element Analysis

A model of the delaminated plate, shown in Fig. 1, was numerically analyzed using a finite element method (ABAQUS 5.5) to study the effect of multiple delaminations on the postbuckling and failure mechanisms. The failure mechanism was discussed through energy release rates along the delamination edges. Plates without a delamination and with multiple delaminations of diameters 10, 20, and 30 mm were considered. Five delaminations were assumed in the analysis, corresponding to the specimens used in the experiment.[12] Convergence of the solution was not easily attained in the postbuckling phase due to a contact problem described later. Introduction of orthotropy frequently disturbed the convergence of the solution. Considering that the effect of elastic properties in the thickness direction on compressive behavior is usually secondary, the material properties were assumed to be isotropic ($E = 41.9$ GPa, $\nu = 0.31$). To obtain the energy release rates G_I, G_{II}, and G_{III} along the delamination edges, a three-dimensional, isoparametric, 20-node block element (C3D20 in the ABAQUS manual) was chosen for the present analysis. Figure 2 shows a typical finite element mesh. Because the plate was divided into six layers in the thickness direction,

Presented as Paper 94-1368 at the AIAA/ASME/ASCE/AHS/ASC 35th Structures, Structural Dynamics, and Materials Conference, Hilton Head, SC, April 18–20, 1994; received May 20, 1997; revision received March 1, 1998; accepted for publication March 27, 1998.

*Professor, Department of Mechanical Engineering, Faculty of Science and Technology, 7-1 Kioi-cho Chiyodaku. E-mail: suemasu@hoffman.cc.sophia.ac.jp. Member AIAA.

†Graduate Student, Department of Mechanical Engineering, Faculty of Science and Technology, 7-1 Kioi-cho Chiyodaku.

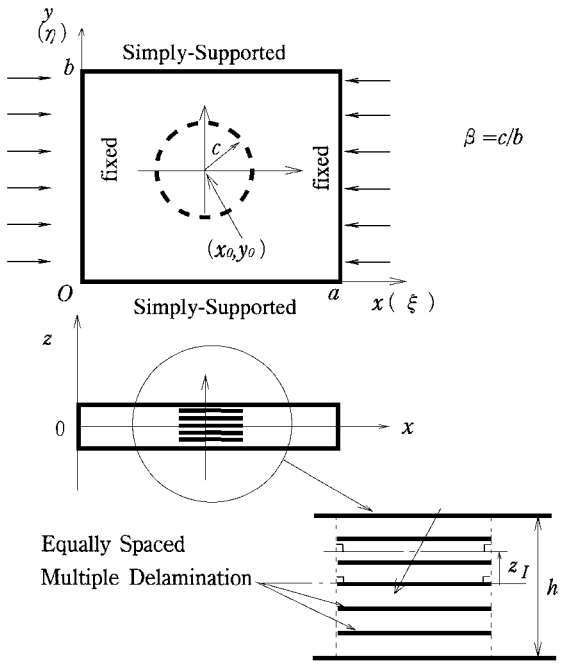

Fig. 1 Schematic of a rectangular laminate with circular multiple delaminations.

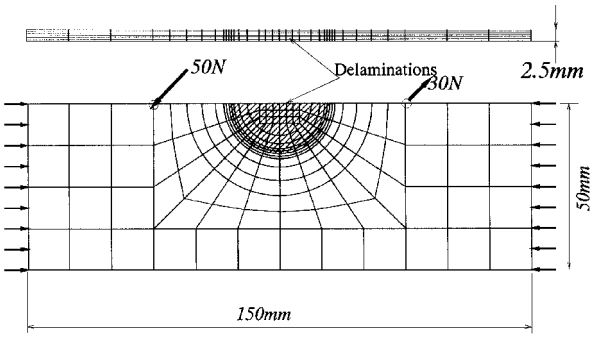

Fig. 2 Schematic of a typical finite element mesh, $c = 30$ mm.

the aspect ratio of the element was quite large. However, no significant problem was encountered for the present analysis through use of such a thin block element. Because the deformation was symmetrical about the centerline parallel to the loading direction, only half of the plate was analyzed. The displacement of the node normal to the surface was constrained on the cross section of the symmetry to satisfy the symmetric condition. On the simply supported edge, the out-of-plane displacement of the centerline of the side boundary was constrained. At one of the fixed ends, the displacement in the loading direction was set to zero, whereas at the other end a uniform displacement in the loading direction was applied. Instead of considering an initial imperfection, small concentrated loads were applied at two points on the centerline of the plate, as shown in Fig. 3. Because of this initial transverse load, the plate deflected by approximately $\frac{1}{20}$ of its thickness.

The present calculation was quite difficult and needed a large numerical effort inasmuch as not only a geometrical nonlinearity but also the contact problem on all the delaminated surfaces must be considered in the three-dimensional finite element analysis. Compressive behavior of the plate was calculated by increasing the uniform displacement of the loading edge with an increment that was small enough to ensure convergence. The convergence was normally most difficult to achieve at the region just prior to and following buckling. At this load level, contact areas were thought to rapidly change with only a small change in loading due to the very small opening of the delaminations. Thus, the calculation should be initiated from a shape where all delaminations are open and no contact exists.

To consider the contact problem on the delaminated surface, a spring element (SPRING2 in the ABAQUS manual) was used

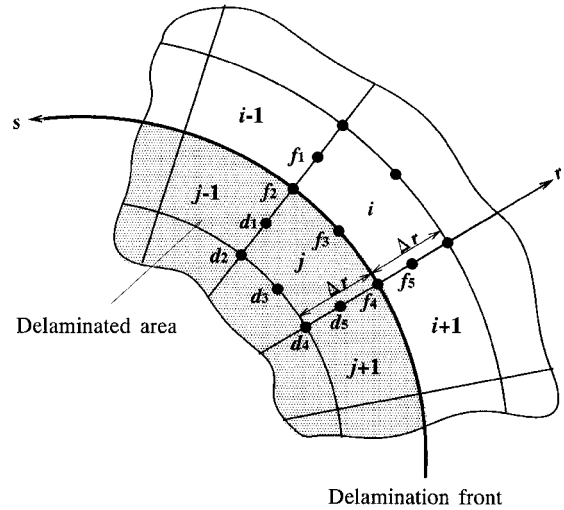

Fig. 3 Schematic showing the nodal forces and relative displacements of the elements at the delamination edge.

between nodes on the upper and lower delaminated surfaces. The element had a large reaction force when the relative displacement in the thickness direction, Δw, was negative and no force when the relative displacement was positive, i.e.,

$$F = \begin{cases} k\Delta w & (\Delta w < 0) \\ 0 & (\Delta w > 0) \end{cases} \tag{1}$$

In the present analysis, the so-called GAP element, which is a special spring element to express a zigzag load-displacement relationship, was not utilized because the GAP element required more computation time and occasionally caused the nonconvergence of solution inasmuch as the contact process in a multiply delaminated plate was particularly sensitive during postbuckling. The present spring element was an approximation of the contact problem and valid when the deflection was moderate.

Energy release rates are obtained using the virtual crack closure technique.[13] Two elements i and j, shown in Fig. 3, are considered at a delamination front. The radial length of both elements must be set equal to derive the energy release rate through the current technique using one calculation. It is necessary to obtain the nodal force f_k of node k ($k = 1, \ldots, 5$) of element i and the relative displacement Δw_k of node k ($k = 1, \ldots, 5$) of element j. Because the nodal force is a sum of the contributions of nodal forces of adjacent elements, the following expression can be used to determine the energy release rate at the element i:

$$G_I = \frac{1}{2\Delta r \Delta s_i}\left[\frac{\Delta s_i}{\Delta s_{i-1} + \Delta s_i}(f_1\Delta w_1 + f_2\Delta w_2) + f_3\Delta w_3 + \frac{\Delta s_i}{\Delta s_i + \Delta s_{i+1}}(f_4\Delta w_4 + f_5\Delta w_5)\right] \tag{2}$$

where Δr and Δs_i are the radial and circumferential lengths of element i, respectively. Though only the method of how to calculate the mode I energy release rate is included here, the other energy release rates can be calculated in a similar manner. The nodal forces were easily obtained by setting very stiff spring elements of no length in three directions between the nodes of the block elements above and below the delaminated surface at the points f_i in Fig. 3. Relative displacements in the delaminated portions can be also monitored conveniently using very flexible spring elements. The nonlinear spring element mentioned earlier could be used to monitor out-of-plane relative displacement, although two very flexible spring elements were inserted at each point d_i in Fig. 3 to derive two in-plane relative displacements.

III. Results and Discussion

The effect of orthotropic properties was studied first for the undelaminated plate. The in-plane elastic properties of the orthotropic

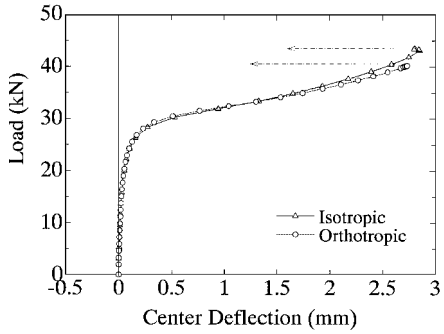

Fig. 4 Effect of orthotropy on the load and center deflection curve for a laminated composite.

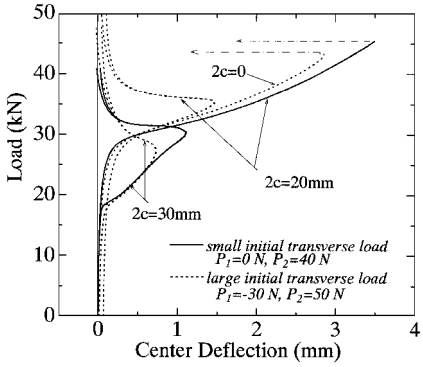

Fig. 5 Effects of the initial transverse load on the compressive behavior of the delaminated plates.

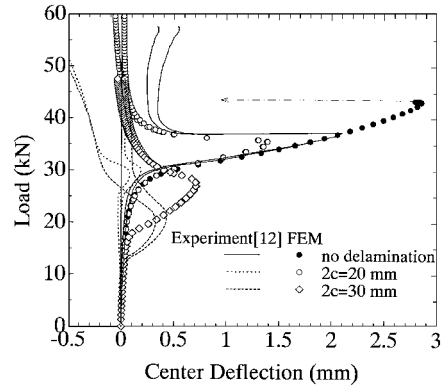

Fig. 6 Comparison of the relationship between compressive load and center deflections: curves, experimental results, and symbols, present finite element results.

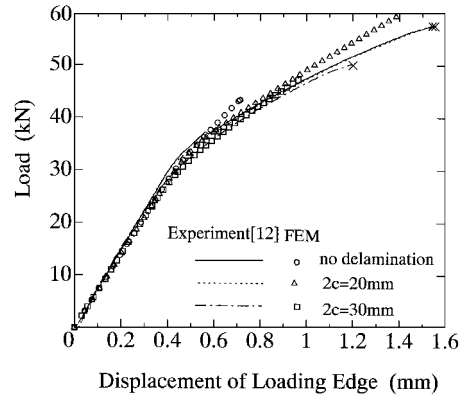

Fig. 7 Comparison of the relationship between compressive load and loading edge displacement: curves, experimental results, and symbols, present finite element results.

model were the same as those of the isotropic one, whereas the out-of-plane Young's modulus E_z and Poisson's ratio v_{xz} of the orthotropic plate were 11.6 GPa and 0.057, respectively. Center deflections for the undelaminated plates are compared in Fig. 4. The solutions farther than those plotted could not be obtained for both cases, probably due to secondary unstable snap-through buckling from symmetric to antisymmetric shape. Because the reaction force for the orthotropic plate was only slightly smaller than that for the isotropic case, and the effect of the low transverse stiffness of the composite plate was not particularly important for the overall compressive problem of the thin plate, it is possible to conclude that the results of the isotropic plate can be used to discuss the reduction in the compressive properties for the composite laminates.

The effect of initial transverse load on the compressive behavior is presented in Fig. 5. When the antisymmetric component was small, the symmetric deformation increased up to a fairly large load level, and then the finite element program was suddenly terminated for the cases of $2c = 0$ and 20 mm because of the lack of convergence of the solution. For the case of $2c = 30$ mm, the plate gradually changed the deformed shape from symmetric to antisymmetric, and the problem of instability did not occur even for the small antisymmetric initial imperfection. The features of the compressive behaviors did not essentially change, though the postbuckling paths looked substantially different, depending on the initial imperfection. Therefore, small initial transverse loads should be adopted to obtain a fundamental result if possible.

The center deflection and loading edge displacements obtained from the experiment and the finite element analyses are compared in Figs. 6 and 7, respectively. The postbuckling path above 43 kN for the undelaminated plate could not be obtained using the current finite element code, probably due to the unstable snap-through secondary buckling as mentioned earlier. The plates with multiple delaminations gradually changed their deformed shapes from symmetric to antisymmetric. The low buckling loads obtained experimentally for the delaminated plates as compared to the analytical results were thought due to a thickness reduction and large local initial imperfection of the delaminated portion as a result of the insertion of Teflon® sheets.[12] Although the plate with $2c = 30$ mm buckled at about 18 kN for the finite element analysis and 14 kN for the experiment, the stiffness reductions were barely visible in the region immediately following the buckling (Fig. 7). The result would suggest that the buckling was only local buckling of the delaminated portion and the remainder of the plate still possessed a load-carrying capacity. The stiffness reduction became appreciable when the load was increased further and, finally, more significant when the center deflection stopped increasing due to secondary buckling. It was found that the delaminations closed during symmetric postbuckling and then started to open slightly as the antisymmetric deformation increased, i.e., symmetric deformation started to decrease. The opening of the delaminations was slightly larger for the experiment compared to the finite element analysis. The initial opening of the delaminations in the test specimens was the order of the thickness of the Teflon sheets and thought to be larger than the finite element analysis. In the present analysis and the experiment described in Ref. 12, the delamination opening was insignificant, although the delamination opening was reported to be observed in postbuckling in the compressive test of the impact-damaged laminate.[8] The delamination opening observed in the compressive test of the impacted laminates, which is, of course, possible, depending on the initial imperfection of the present model, may be attributed to the delamination size changing in the impacted specimen through the thickness direction of the plate (conical distribution of damage). Deformed shapes for the plate with $2c = 30$ mm are given in Fig. 8. The analytical results correlated well with the experimental data, particularly considering the complex influences of the boundary conditions and initial imperfections.

Dimensionless buckling loads are plotted against normalized delamination diameter $2\beta = 2c/b$ in Fig. 9. The buckling loads obtained from the finite element analysis were approximately 3% smaller compared to the Rayleigh–Ritz analysis[12] based on the Kirchhoff hypothesis and 10–15% higher compared to the

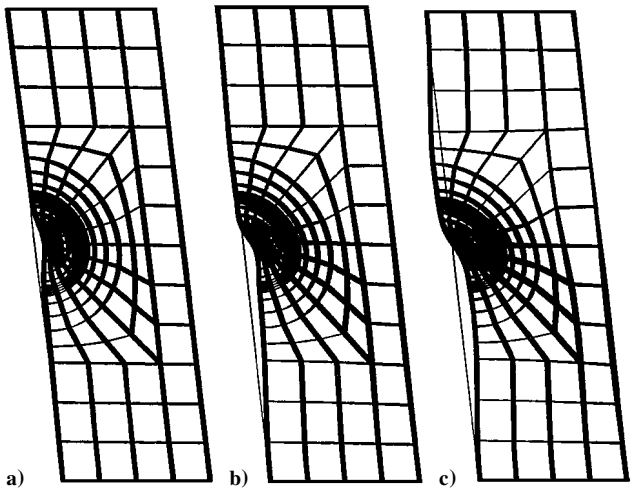

Fig. 8 Deformed shapes of multiply delaminated plates: a) symmetric deformation, $P = 24.1$ kN; b) transient state of the deformation from symmetric to antisymmetric, $P = 31.5$ kN; and c) antisymmetric deformation, $P = 38.8$ kN.

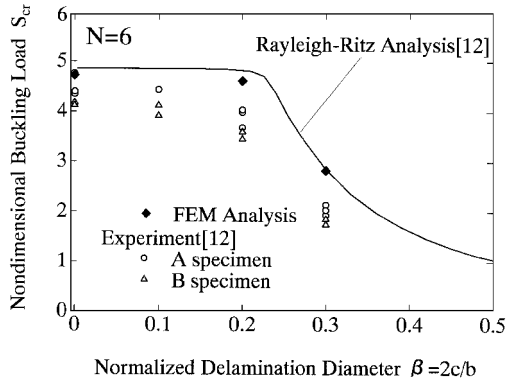

Fig. 9 Nondimensional buckling load $S_{cr} = P_{cr}b/(Eh^3)$ as a function of normalized delamination diameter $2\beta = 2c/b$.

experiment. The low buckling load in the experiment was due to the reasons already mentioned. It is thought that the finite element results may agree well with the experiment when initial imperfection, boundary conditions, and thickness of the delaminated layers were precisely stated.

Inasmuch as the energy release rates were usually maximum at the edge of the center delamination, only distributions for the energy release rates at that region will be discussed. The position of the maximum deflection for the plate with a notable initial antisymmetric component compared to the symmetric one moved away from the plate center, even when the plate was on the symmetric postbuckling path. When the delaminated portion was located at the inclined section of the plate, the G_{III} component became large compared to that of G_{II}, as shown in Figs. 10a and 10b. Figure 10a shows the results for the plate with a larger antisymmetric initial imperfection compared to that of the plate in Fig. 10b. The ratio of the components of energy release rate was found to strongly depend on the position of the delaminations in the global deformed shape.

Distributions of the energy release rates G_I, G_{II}, and G_{III} along the delamination edges are plotted in Figs. 11, 12, and 13, respectively. The value of G_I was almost zero at $P = 25.8$ kN due to closing of the delaminations. As the load increased and the antisymmetric component of the deformation became dominant, G_I increased slightly in the direction transverse to the load. However, the value was still negligible compared to that of G_{III}. Along the symmetric postbuckling path, G_{II} increased linearly with load and became almost symmetric about the centerline. For this case, the value of G_{II} was of the same order as G_{III} because the antisymmetric component existed and was not negligible.

Along the antisymmetric path, G_{II} reduced with increasing load, particularly at the edge of the transverse direction, because the

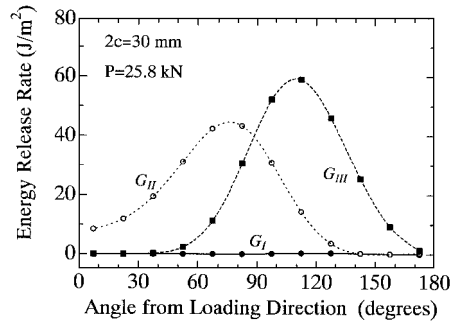

a) $P_1 = 50$ N, $P_2 = 30$ N

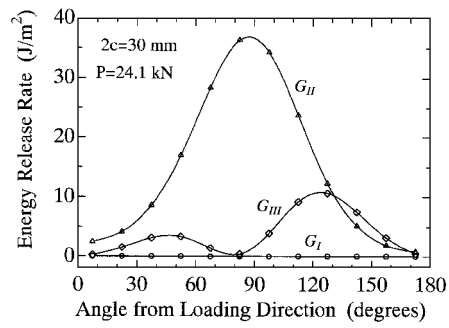

b) $P_1 = 40$ N, $P_2 = 0$

Fig. 10 Effect of initial imperfection on the postbuckling behavior.

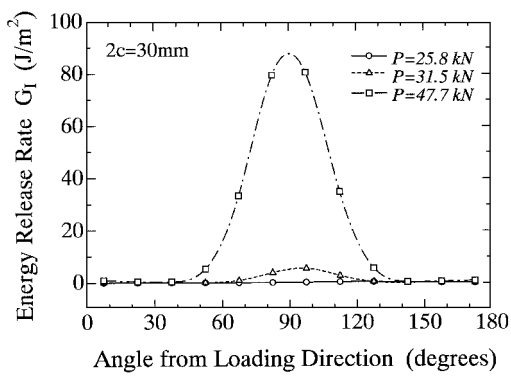

Fig. 11 Distribution of the mode I energy release rate along the delamination edge when $2c = 30$ mm.

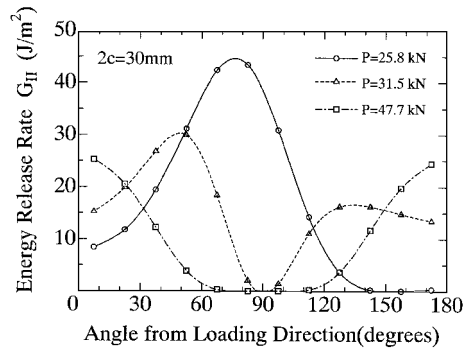

Fig. 12 Distribution of the mode II energy release rate along the delamination edge when $2c = 30$ mm.

deflection along the centerline approached zero. This value was even smaller than that of G_I and was also thought to be negligible. Thus, the value of G_{III} was of most importance. The increase in G_{III} was only slight in the symmetric postbuckling path. However, it grew rapidly with the increase in antisymmetric deformation and exceeded 1000 J/m^2 at the load level of $P = 47.7$ kN. The energy release rate always tended to be maximum at the edge of the direction transverse to the load. These results suggest that the delaminations

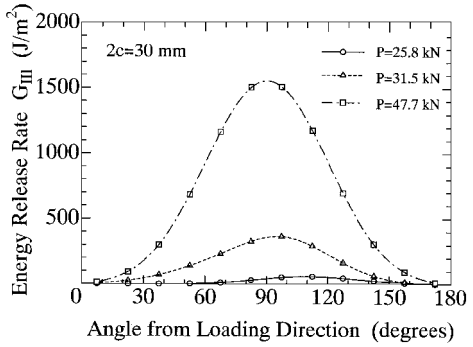

Fig. 13 Distribution of the mode III energy release rate along the delamination edge when $2c = 30$ mm.

should preferably propagate in the transverse direction and agreed well with the experimental findings.[8] The value of 1000 J/m^2 would be a possible G_{III} toughness of the woven CF/epoxy. The failure loads of the laminate with the delaminations of $2c = 30$ mm obtained in the experiment, about 40 kN for B specimen and 53 kN for A specimen,[12] were consistent with the present results, considering the energy release rates obtained from the finite element analysis. Therefore, we may predict the failure load of the laminated composite if we know the value of G_{IIIc}.

IV. Conclusions

Postbuckling paths and the energy release rate distribution were obtained for multiply delaminated plates along the delamination edges using a finite element method. The postbuckling behavior obtained by the present finite element analysis agreed well with experimental results, whereas the failure loads due to the instability of delaminations were consistent with those inferred from the value of energy release rates obtained. The following conclusions are noted.

1) Plates with multiple delaminations buckle with a symmetric shape. However, their shape changes gradually with increasing load from symmetric to antisymmetric. If the plate is not thick, then the antisymmetric deformation must be considered to discuss the CAI problem.

2) The compressive strength of the composite plate with multiple delaminations, whose failure is initiated by delamination propagation in the transverse direction, may be well predicted by obtaining the energy release rate at the transverse direction of the delamination.

3) When the plate is thick and small postbuckling deformation needs to be considered, the G_{II} component tends to be important in the transverse direction of the delamination. However, the relative values of G_{II} and G_{III} strongly depend on the position of the delamination in the global deformed shape. When the postbuckling deformation is large and antisymmetric, G_{III} becomes dominant among the three components.

Acknowledgments

The present research was supported by Ministry of Education, Science and Culture, Japan, Grant Aid for Scientific Research (C) 06650765 and Iketani Science and Technology Foundation Grant 061014-BA. The English has been kindly revised by I. J. Davies, Visiting Scientist of Sophia University.

References

[1]Wang, S. S., Zahlan, N. M., and Suemasu, H., "Compressive Stability of Delaminated Random Short-Fiber Composite, Part I—Modeling and Methods of Analysis," "Part II—Experimental and Analytical Results," *Journal of Composite Materials*, Vol. 19, July 1985, pp. 296–333.

[2]Suemasu, H., Omata, K., Majima, O., and Hayashi, K., "Finite Element Analysis of Compressive Behaviors and Delamination Crack Instability of Multiply Delaminated Cross-Ply Laminates," *Journal of Japan Society for Aeronautical and Space Sciences*, Vol. 43, No. 500, 1995, pp. 513–519.

[3]Davidson, B. D., and Krafchak, T. M., "A Comparison of Energy Release Rates for Locally Buckled Laminates Containing Symmetrically and Antisymmetrically Located Delaminations," *Journal of Composite Materials*, Vol. 29, No. 6, 1994, pp. 700–715.

[4]Lee, J., Guldal, Z., and Griffin, O. H., Jr., "Postbuckling of Laminated Composites with Delaminations," *AIAA Journal*, Vol. 33, No. 10, 1995, pp. 123–128.

[5]Whitcomb, J. D., and Shivakumar, K. N., "Strain-Energy Release Rate Analysis of Plates with Postbuckled Delaminations," *Journal of Composite Materials*, Vol. 23, July 1989, pp. 714–734.

[6]Shahwan, K. W., and Waas, A. A., "A Mechanical Model for the Buckling of Unilaterally Constrained Rectangular Plates," *International Journal of Solids and Structures*, Vol. 31, No. 1, 1994, pp. 23–37.

[7]Klug, J., Wu, X. X., and Sun, C. T., "Efficient Modeling of Postbuckling Delamination Growth in Composite Laminates Using Plate Elements," *AIAA Journal*, Vol. 34, No. 1, 1996, pp. 178–184.

[8]Ishikawa, T., Sugimoto, S., Matsushima, M., and Hayashi, Y., "Some Experimental Findings in Compression after Impact (CAI) Tests of CF/PEEK(APC-2) and Conventional CF/Epoxy Flat Plates," *Composite Science and Technology*, Vol. 55, No. 4, 1995, pp. 349–363.

[9]Lee, S. M., "Compression-After-Impact of Composites with Toughened Matrices," *SAMPE Journal*, Vol. 22, No. 2, 1986, pp. 64–68.

[10]Prichard, J. C., and Hogg, P. J., "The Role of Impact Damage in Post-Impact Compression Testing," *Composites*, Vol. 21, No. 6, 1990, pp. 503–511.

[11]Dost, E. F., Ilcewicz, W. B., Avery, W. B., and Coxon, B. R., "Effects of Stacking Sequence on Impact Damage Resistance and Strength for Quasi-Isotropic Laminates," *Composite Materials: Fatigue and Fracture*, ASTM STP 1110, American Society for Testing and Materials, 1991, pp. 476–500.

[12]Suemasu, H., Kumagai, T., and Gozu, K., "Compressive Behavior of Multiply Delaminated Composite Laminates Part 1: Experimental and Analytical Development," *AIAA Journal*, Vol. 36, No. 7, 1998, pp. 1279–1285.

[13]Shivakumar, K. N., Tan, P. W., and Newman, J. C., "A Virtual Crack-Closure Technique for Calculating Stress Intensity Factors for Cracked Three Dimensional Bodies," *International Journal of Fracture*, Vol. 36, 1988, pp. R43–R50.

A. M. Waas
Associate Editor